JOURNAL OF Materials CHEMISTRY

# A study of the mechanism of the reaction of trimethylgallium with hydrogen selenide

**Nicholas Maung,*[a] Guanghan Fan,[b] Tat-Lin Ng,[a] John O. Williams[a] and Andrew C. Wright[a]**

[a]*Advanced Materials Research Laboratory, North East Wales Institute, Plas Coch, Mold Road, Wrexham, Wales, UK LL11 2AW. E-mail: n.maung@newi.ac.uk*
[b]*Institute of Quantum Electronics, South China Normal University, Guangzhou, Guangdong, 510631, Peoples Republic of China*

***Received 6th April 1999, Accepted 29th June 1999***

A study of the pre-deposition room temperature gas-phase reactions involved in the growth of $Ga_2Se_3$ (and/or GaSe) using trimethylgallium ($GaMe_3$) and hydrogen selenide ($H_2Se$) was undertaken, using a simple mass spectrometric sampling system on a conventional atmospheric pressure MOCVD reactor. The experimental studies were complemented by theoretical quantum chemical calculations which were used to predict the reaction thermochemistry and kinetics of the proposed reaction scheme. We have shown that the gas phase reaction of the $GaMe_3$–$H_2Se$ mixture can be described by a simple reaction mechanism with no need for the participation of a stable Lewis acid–base adduct, although a transient adduct type species may be involved. The effect of the room temperature reaction of $GaMe_3$ with $H_2Se$ on the growth mechanism of $Ga_2Se_3$/GaSe and its role in determining epilayer morphology and microstructure are also discussed.

## Introduction

Epitaxial films of the cubic wide band gap III–VI (13–16) semiconductor gallium selenide, $Ga_2Se_3$, have potential applications in short-wavelength optoelectronic devices, *e.g.* green–blue light-emitting diodes and a number of workers have investigated its materials properties.[1,2]

The MOCVD growth of $Ga_2Se_3$ has been carried out using trimethylgallium ($GaMe_3$) with hydrogen selenide ($H_2Se$).[3] Although $Ga_2Se_3$ with adequate structural properties could be obtained,[4–6] a severe pre-deposition gas phase reaction occurs with these reagents, compromising the compositional uniformity and surface morphology of the epilayers. More recent attempts to improve $Ga_2Se_3$ materials quality have resulted from the use of alternative organoselenium reagents[7,8] and this has been shown to enhance the structural quality of the $Ga_2Se_3$ films.[6]

Although the quality of epitaxial films utilised in thin film technologies is of critical importance there is little or no detailed knowledge of the growth process. Other than the overall stoichiometry of the reaction, in the case of $Ga_2Se_3$ growth from $GaMe_3$ and $H_2Se$,

$$2GaMe_3 + 3H_2Se \rightarrow Ga_2Se_3 + 6CH_4 \qquad (R1)$$

little is known about the participation of any intermediate species that may be created and subsequently destroyed in the growth process.[8] The ability of individual $GaMe_3$ molecules to form complexes with Lewis bases is well documented[9] and Piocos and Ault have investigated the formation of molecular complexes of trimethylgallium with group V hydrides[10–12] and dimethylzinc with group VI hydrides[13] using matrix isolation and cryogenic thin film techniques. We have published *ab initio* molecular orbital and density functional theory (DFT) calculations describing the geometries, harmonic frequencies and binding energies of the gallane and $GaMe_3$ adducts with $H_2Se$;[14] the major finding being that such species are not expected to be stable intermediates under MOCVD growth conditions.

The work described here was undertaken in an effort to understand the pre-deposition gas phase reactions involved in the growth of $Ga_2Se_3$ using $GaMe_3$ and $H_2Se$ and to obtain, if possible, kinetic data which could be incorporated in a model of the pre-deposition reaction. Mass spectrometry has been used extensively to study reaction chemistry in MOCVD[3,8,15] although little of the work has led directly to an improvement in the understanding of the relevant reaction kinetics due to the complex nature of the processes involved. In this work mass spectrometry was chosen to study gas phase reactions since it has been used successfully in the past in elucidating the reaction kinetics of the triethylindium/arsine system,[16–17] a precursor combination which undergoes a similiar pre-deposition reaction on mixing.

## Experimental

A differentially pumped mass spectrometer system utilising a sampling tube *via* a leak valve has been installed on a conventional atmospheric pressure MOCVD reactor for studying the room temperature interactions between the reactant gases under typical growth conditions. The basic layout of the sampling system has been described previously.[3] The differentially pumped sampling system was designed to minimise the time that the sampled gases are subjected to gas phase interactions *en route* to the ionisation chamber of the mass spectrometer. We have considered the possibility that surface catalysed reactions in the sampling tube may have a significant effect on the interpretation of our results due to the large surface/volume ratio ($\approx 5$) of the sampling tube. We note, however, that most other workers[15,16] used concentrations well in excess of those used for conventional epitaxial growth thus favouring gas phase processes over those that take place at the surface. Moreover, our work shows that the extent of reaction changes significantly as a function of probe position in the reactor even though the length of the probe is unaltered, see Fig. 1. Thus, we do not expect that surface catalysis plays a significant role in the reactions leading to the formation of involatile products.

During the growth of $Ga_2Se_3$ (and/or GaSe) we have noted the formation of a white/buff coloured deposit of possibly polymeric material with a Ga : Se ratio of 1 : 1 [analysed by energy dispersive analysis by X-rays (EDAX) in a transmission electron microscope] in the coolest parts of the reactor chamber, *viz.* on the quartz reactor chamber tube liner in

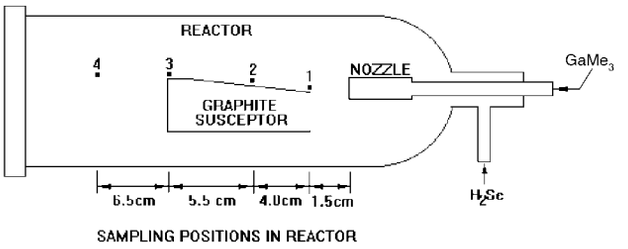


**Fig. 1** Schematic diagram of reactor indicating sampling probe positions.

front of and at the rear of the susceptor, on the outside of the $GaMe_3$ inlet nozzle.[3] The inside surface of the sampling tube becomes similarly coated during the sampling process as became evident on examination after completing the experiment. The white/buff coloured material that deposits on the walls is removable using simple methods (*aqua regia*). The crystallinity of the deposit was evaluated by electron diffraction measurements but no electron diffraction spots were observed, indicating that the final reaction product is amorphous. It is unstable under the electron beam unlike GaSe which is stable under electron irradation. The white/buff coloured deposit is stable under dry dihydrogen in the MOCVD reactor but slowly changes to an orange/brown colour with time on removal from the growth system, even when stored in a desiccator. The moisture/air sensitivity of the final reaction product means that we were unable to extract a 'pristine' sample of the deposit from the reactor and conduct meaningful analysis using conventional techniques such as elemental analysis, thermal gravimetric analysis (TGA), differential scanning calorimetry (DSC), solid state NMR and IR spectroscopy, since we did not carry out the experiments in a dry glovebox interfaced directly to the reactor chamber.

III–VI MOCVD growth was carried out with a cold wall reactor resulting in a highly non-uniform temperature profile near the susceptor. The decomposition studies presented here were therefore all conducted with a cold susceptor since the reaction occurs rapidly at room temperature and mixing of the reagents occurs nominally at *ca.* 300 K. Under these circumstances heating the susceptor introduces unnecessary complications in the analysis and interpretation of the data. In all cases, $GaMe_3$ alone in dihydrogen was admitted into the reactor initially in order to allow sufficient time for the $Me_2Ga^+$ signal to achieve a steady state prior to the introduction of $H_2Se$ into the reactor (this took around 1 h). The VI/III ratio was increased incrementally by increasing the flow of $H_2Se$ into the reactor while keeping the flow of $GaMe_3$ constant.

Typical $Ga_2Se_3$ (and/or GaSe) growth parameters we used in our study were a $GaMe_3$ bath temperature of $-12\,^{\circ}C$ and a flow of 10 $cm^3$ (STP) $min^{-1}$ of hydrogen through the bubbler to give a $GaMe_3$ molar flux of $2.46\times10^{-5}$ mol $min^{-1}$. The input VI/III molar ratio was adjusted between 1 and 4 by changing the $H_2Se$ flow (5% in hydrogen) between 5.2 and 43.2 $cm^3$ (STP) $min^{-1}$ diluted in a total hydrogen carrier flow of 900 $cm^3$ (STP) $min^{-1}$.

## Results and discussion

Reactions between $MR_n$ species [M = group II (12) or III (13) metal and R = alkyl] and hydrides of the form $XH_n$ [X = group V (15) or VI (16) element] generally lead to metastable reaction products which react further to yield polymeric materials by the elimination of a stable alkane. Indeed, the elimination of methane and formation of a full covalent bond to a group 13 metal is well documented[8,9] when the second component is a group 15 hydride and one might expect the group 16 hydrides to behave similarly. One objective of our study was to obtain kinetic data for the $GaMe_3$–$H_2Se$ reaction, which we have been using to grow $Ga_2Se_3$, and to use these data to come to some realistic conclusions about the reaction mechanism. We have also used quantum chemical methods to make predictions as to the extent of the pre-deposition reaction between $GaMe_3$ and $H_2Se$.

The fragmentation patterns of the reactant species were first determined individually. We previously determined[3] the patterns for $GaMe_3$ and $H_2Se$, respectively, and the ion intensities were found to be linear, down to *ca.* 10% of the $GaMe_3$ pressures used in this study. In our present study, a fragment of the metal–organic compound with a strong signal, in the case of $GaMe_3$ the $Me_2Ga^+$ daughter fragment with *m/z* 99, was monitored as a function of time as the $H_2Se$ was introduced into the reactor. Changes in its magnitude can be attributed directly to reactions that take place between $GaMe_3$ and $H_2Se$ as the total dihydrogen flow was fixed. The inlet gas stream contained a small amount of Ar as an internal standard during all experiments to allow for data normalisation and to avoid artifacts associated with gas expansion.

Two complications arise in the interpretation of the mass spectrometric data. First, the observed turn-on and turn-off transients for the metal–organic species are a strong function of adsorption and desorption phenomena in the reactor and in the mass spectrometer, and depend on the past history of the sampling system. This is especially true in the present case. By way of example, Fig. 2 shows a series of plots for $Me_2Ga^+$ fragments, taken in a clean system (reactor and sampling tube) for a constant input partial pressure of $GaMe_3$. Note that the immediate drop in the signal, once the $H_2Se$ is introduced, is modified by adsorption/desorption phenomena from run to run, but that the steady-state extent of reaction is the same in all cases. In order to determine the reaction rate, it was necessary to determine the steady-state extent of reaction at various distances down the reactor. This was related to the time the reactants have spent together and the rate constants were determined by reference to the extent of reactant depletion with time.

A second potential complication arises from the nature of the detection system. In order to study the reaction of the various organometallic compounds, we must monitor a daughter fragment which produces a large signal to ensure sufficient sensitivity. The largest daughter fragment is usually the dialkyl metal species for the group III metal–organic compounds. If the product formed by the reaction of $GaMe_3$ with $H_2Se$ also fragments to the same dialkyl metal species, then its signal will not represent the amount of unreacted compound only, obviously resulting in a significant underestimate of the extent of reaction.

In the case of the $GaMe_3$–$H_2Se$ reaction, the dimethylgal-

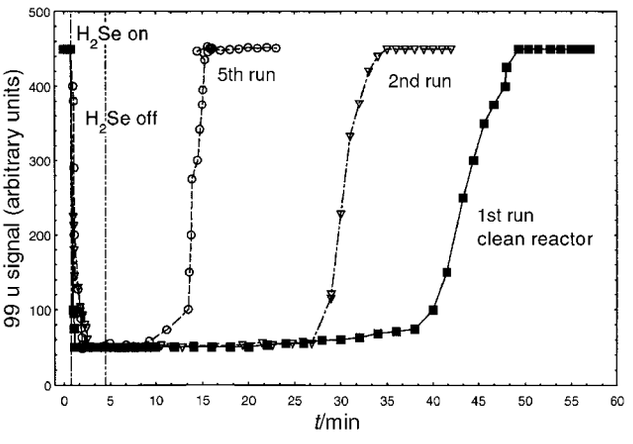


**Fig. 2** Behaviour of dimethylgallium fragment ion signal upon the addition of $H_2Se$ gas illustrating the system memory effect.

lium ($Me_2Ga^+$) fragment was found to drop to approximately zero under conditions of large $H_2Se$ excess, indicating that the reaction product does not fragment to $Me_2Ga^+$. We can thus conclude that the $Me_2Ga^+$ signal represents the concentration of $GaMe_3$ remaining in the reactor.

Fig. 3 shows the amount of $GaMe_3$ remaining in the reactor at steady state as a function of distance from the inlet region of the reactor. This was measured by comparing the value of the $Me_2Ga^+$ fragment both before and after the addition of $H_2Se$, as a function of the input VI/III molar ratio at various distances (probe positions) from the inlet region. Using the value of the average gas velocity at 300 K, the residence time in the mixing region may be estimated.

The data taken at 5.5 and 11 cm from the reactor inlet are very similar and seem to be asymptotically approaching the VI/III molar ratio axis. It is clear that the $GaMe_3$ is fully consumed, even for $H_2Se$ concentrations only twice that of $GaMe_3$ at distances greater than 5.5 cm (probe position 2) from the reactor inlet. From this we can conclude that the reaction has gone to completion after the reactants have travelled 5.5 cm down the reactor, *i.e.* within *ca.* 6 s of mixing for VI/III molar ratios in excess of unity. This evidence strongly suggests that the reaction product forms from a 1 : 1 ratio of $GaMe_3 : H_2Se$. It is clear from Fig. 3 that at a distance of 17.5 cm (probe position 4), *i.e.* within *ca.* 12 s of mixing, from the reactor inlet, the reaction has gone virtually to completion for $GaMe_3 : H_2Se$ ratios in excess of 1 : 1.

The growth of high quality $Ga_2Se_3$ at low temperatures using $GaMe_3$ and $H_2Se$ taken together with the observation of the extensive room temperature parasitic gas phase reaction and the production of white/buff coloured deposits, clearly indicates that different mechanisms control the deposition of $Ga_2Se_3$ from this precursor combination compared with Se metal–organic sources. Since, the reaction appears to be moderately fast and is essentially complete on adding the $H_2Se$ to the $GaMe_3$, we propose that the reaction must be gas phase.

A number of possible mechanisms can be proposed based on the experimental data presented above. The initiation step

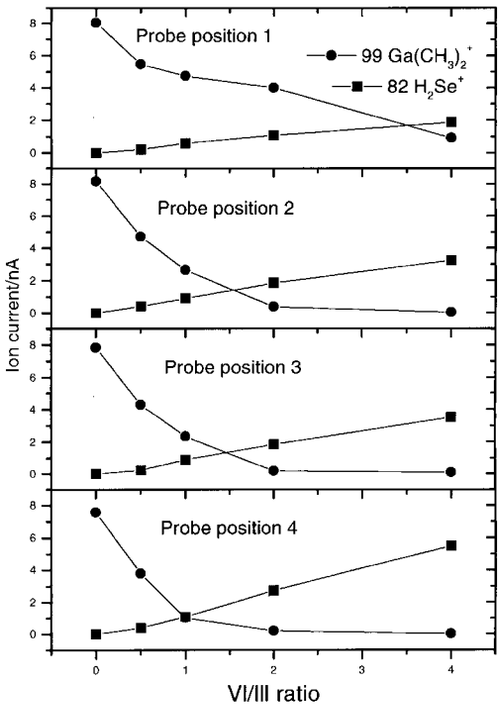


**Fig. 3** Steady state dimethylgallium and $H_2Se$ ion signals as a function of VI/III ratio and sampling probe position in the reactor at room temperature.

cannot be the unimolecular decomposition of $GaMe_3$ since this would require breaking the strong $Me_2Ga$–Me bond[18] which requires 61 kcal $mol^{-1}$ while the available thermal energy at room temperature is $<1$ kcal $mol^{-1}$. We present three possible reaction schemes which differ primarily in the nature of the initial step. The first, mechanism I, involves the formation of an $Me_3Ga{\cdot}SeH_2$ adduct between $GaMe_3$ and $H_2Se$ (R2a) which then undergoes intramolecular elimination of methane (R2b). The other two pathways involve H atom bimolecular abstraction processes which proceed either *via* a stable intermediate, $Me_2Ga$–SeH (R2c), or by direct formation of radicals and products (R2d). In each case the initial step is followed by either the sequential methane elimination reaction (R3) involving intramolecular elimination of methane or by direct reaction of radical species (R4). The final step may be formation of the monoselenide (R5) and/or polymerisation of the unsaturated methylgallium selenide species (R6):

Mechanism I

Adduct formation reaction

$$GaMe_3+H_2Se \leftrightarrow Me_3Ga{\cdot}SeH_2 \quad \text{(R2a)}$$

Direct elimination of methane from the adduct

$$Me_3Ga{\cdot}SeH_2 \rightarrow Me_2Ga-SeH+CH_4 \quad \text{(R2b)}$$

Mechanism II

Bimolecular H abstraction reaction

$$GaMe_3+H_2Se \rightarrow Me_2Ga-SeH+CH_4 \quad \text{(R2c)}$$

Mechanism III

Bimolecular H abstraction and radical formation reaction

$$GaMe_3+H_2Se \rightarrow Me_2Ga^{\cdot}+{}^{\cdot}SeH+CH_4 \quad \text{(R2d)}$$

Subsequent reaction steps:

Mechanism I and II

$$Me_2Ga-SeH \rightarrow MeGa{=}Se+CH_4 \quad \text{(R3)}$$

Mechanism III

$$Me_2Ga^{\cdot}+{}^{\cdot}SeH \rightarrow MeGa{=}Se+CH_4 \quad \text{(R4)}$$

The final competing steps common to all three mechanisms are:

Deposition of GaSe

$$MeGa{=}Se \rightarrow GaSe+{}^{\cdot}CH_3 \quad \text{(R5)}$$

and/or

Polymerisation

$$n\text{MeGa}{=}\text{Se} \rightarrow (\text{MeGa–Se})_n \quad \text{(R6)}$$

Since it is difficult to obtain unambiguous mechanistic information on the reaction of $GaMe_3$ and $H_2Se$, we have carried out theoretical calculations on the intermediate species $Me_2Ga$–SeH and MeGa=Se to determine reaction thermochemistry and activation barriers using both conventional Hartree–Fock[19] and density functional theory (DFT).[20,21] We have already published analagous data for $GaMe_3$, $H_2Se$ and $Me_3Ga{\cdot}SeH_2$.[14] All DFT calculations were performed using the GAUSSIAN 94 program package[22] on a Silicon Graphics R10000 workstation. The SPARTAN 4.1.2 electronic structure program[23] was used to generate starting structures and to animate vibrational frequencies. Geometry optimisation, critical point characterisation (all calculated structures were found to correspond to true energy minima), normal mode analysis (vibrational frequencies) and thermodynamic calculations[24–27] were carried out using the default GAUSSIAN convergence criteria.[28,29] All of the geometries for the molecules studied were fully optimised without using symmetry or structural constraints. Restricted Hartree–Fock (RHF) theory was used as an uncorrelated reference and hybrid-density functional theory B3LYP (Becke's three parameter

Table 1 Total energies ($E_h$[a]) for all species involved in the proposed reaction mechanisms calculated at the hybrid-DFT (B3LYP) level. DFT calculations were performed using the GAUSSIAN 94 program package[22] and the 6-311G(d,p) basis set[28,29]

| Molecular species | Energy | ZPE | Thermal energy at 298 K | Energy at 298 K |
|---|---|---|---|---|
| Ga | −1924.824374 | — | 0.001416 | −1924.822958 |
| $GaMe_3$ | −2044.650990 | 0.105736 | 0.112741 | −2044.538249 |
| $GaMe_2^{\cdot}$ | −2004.680849 | 0.069391 | 0.075644 | −2004.605204 |
| GaMe | −1964.775394 | 0.033299 | 0.036865 | −1964.738529 |
| $CH_3$ | −39.853757 | 0.029574 | 0.032641 | −39.821116 |
| $CH_4$ | −40.533743 | 0.044585 | 0.047454 | −40.486289 |
| $H_2Se$ | −2402.752566 | 0.013471 | 0.016331 | −2402.736235 |
| $HSe^{\cdot}$ | −2402.117182 | 0.005443 | 0.007804 | −2402.109378 |
| $Me_2Ga–SeH$ | −4406.924229 | 0.079069 | 0.086869 | −4406.837360 |
| $(MeGa–Se)_2$ | −8732.811602 | 0.093248 | 0.101677 | −8732.709925 |
| GaSe | −4326.431740 | 0.000698 | 0.003471 | −4326.428269 |
| MeGa=Se | −4366.391769 | 0.036791 | 0.041755 | −4366.350014 |
| $Me_3Ga–SeH_2$ | −4447.409655 | 0.121702 | 0.133158 | −4447.276497 |
| $Me_3Ga–SeH_2$(TS) | −4447.382288 | 0.120541 | 0.131454 | −4447.250834 |

[a] $E_h = 627.5095$ kcal mol$^{-1}$.

exchange functional with the Lee–Yang–Parr (LYP) gradient-corrected correlation functional) method were used with the 6-311G(d,p) basis set. Since scale factors for B3LYP/6-311G(d,p) have not yet been established, the zero-point and thermal energies were used without scaling.[29]

The computed hybrid DFT energies of all the reactants and products described in mechanism I, II and III, are shown in Table 1. Since, Hartree–Fock theory is well known[19] to poorly describe bond forming and bond breaking processes no data computed at the UHF/6-311G(d,p) level is presented here. The computed enthalpy and entropy changes along with the equilibrium constants for the various reactions in the proposed mechanisms are shown in Table 2. The net enthalpy change for the three mechanisms will clearly be identical and, overall, they are exothermic by 36.4 kcal mol$^{-1}$.

Although the equilibrium constant calculated at the hybrid DFT B3LYP/6-311G(d,p) level, at 300 K is small ($10^{-5.4}$) indicating that gas-phase formation of a stable adduct, $Me_3Ga{\cdot}SeH_2$, from $GaMe_3$ and $H_2Se$, (R2a), is not favoured, mechanism I cannot be discounted as a significant pathway for removal of $GaMe_3$. Clearly, although formation of the $Me_3Ga{\cdot}SeH_2$ complex is not energetically favourable because the potential surface is very shallow, if the lifetime of the $Me_3Ga{\cdot}SeH_2$ collision complex is longer than the lifetime of the $Me_3Ga{\cdot}SeH_2$ transition state (TS), then it is possible for the $Me_2Ga–SeH$ intermediate to be formed either from a combination of (R2a)+(R2b) or directly from (R2c) since the two paths effectively become coincident.

The first step in mechanism III is endothermic by 46 kcal mol$^{-1}$ and this is consistent with the need to break the $Me_2Ga–Me$ bond. Mechanism III is therefore not kinetically accessible at 300 K since the rate of the initial step (R2d) is very small, *i.e.* $E(\text{thermal})_{300K} \ll \Delta H_{(R2d)}$.

The first step in mechanism II is exothermic by 31 kcal mol$^{-1}$, so that some of the exoergicity will be available to the $Me_2Ga–SeH$ intermediate and promote further reaction to the final GaSe/polymer products.

The transition state is located closer to the reactant side of the potential energy surface in agreement with Hammond's postulate,[27] since the activation barrier lies only 17.3 kcal mol$^{-1}$ above the reactants ($\Delta H^{\ddagger} = 16.1$ kcal mol$^{-1}$). This barrier is a factor of four lower than that estimated for simple homolytic $Me_2Ga–Me$ bond fission at the B3LYP/6-311G(d,p)//B3LYP/6-311G(d,p) level (*ca.* 70 kcal mol$^{-1}$). The strained four-centred cyclic transition state contains Ga–Se–H–C bonds in the process of forming and breaking (Fig. 4), and the reaction coordinate is a vibrational mode in which the Ga–Se and C–H bonds are decreasing in length while the Se–H and Ga–C bonds are lengthening. The imaginary frequency at $1073i$ cm$^{-1}$ indicates that the transition state is quite tightly bound. The reaction leading to formation of $Me_2Ga–SeH$ may be categorised as a concerted process initiated by the oxidative addition of $H_2Se$ to $GaMe_3$, followed by reductive elimination of methane. Since the collision frequency for a 1 : 1 mixture of $GaMe_3$ and $H_2Se$ at the mol fractions employed in the experiments at 298 K and 1 atmosphere pressure is *ca.* $10^{22}$ cm$^{-3}$ s$^{-1}$ the rate constant for reaction (R2c) would have an upper limit of *ca.* $10^{9}$ cm$^{-3}$ s$^{-1}$, ignoring any steric factors, and this reproduces the observed $GaMe_3$ decay profile. The importance of tunneling effects on the transfer of the hydrogen atom from $H_2Se$ to $GaMe_3$ was estimated using the Wigner tunneling correction factor,[30] and resulted in less than

**Table 2** Computed enthalpies of reaction, entropies of reaction and equilibrium constants ($K$) for mechanism I, mechanism II and mechanism III calculated at the hybrid-DFT (B3LYP) level. DFT calculations were performed using GAUSSIAN 94[22] and the 6-311G(d,p) basis set[28,29]

| | Reaction | Enthalpy/kcal mol$^{-1}$ | Entropy/cal mol$^{-1}$ K$^{-1}$ | $K$ |
|---|---|---|---|---|
| Mechanism I | (2a) | −1.3 | −29.1 | $10^{-5.4}$ |
| | (2b) | −29.6 | 34.1 | $10^{29.1}$ |
| | (3) | 0.7 | 30.6 | $10^{6.2}$ |
| | (5) | 63.1 | 37.3 | $10^{-38.1}$ |
| | (6) | −6.2 | −52.4 | $10^{-6.9}$ |
| | Net (R2a)+(R2b)+(R3)+(R6) | −36.4 | | |
| Mechanism II | (2c) | −30.9 | 5.0 | $10^{23.7}$ |
| | Net (R2c)+(R3)+(R6) | −36.4 | | |
| | Transition state formation ($\Delta H^{\ddagger}$) | 16.1 | −4.3 | $10^{-12.7}$ |
| Mechanism III | (2d) | 46.2 | 41.8 | $10^{-24.7}$ |
| | (4) | −76.4 | −6.2 | $10^{54.6}$ |
| | Net (R2d)+(R4)+(R6) | −36.4 | | |

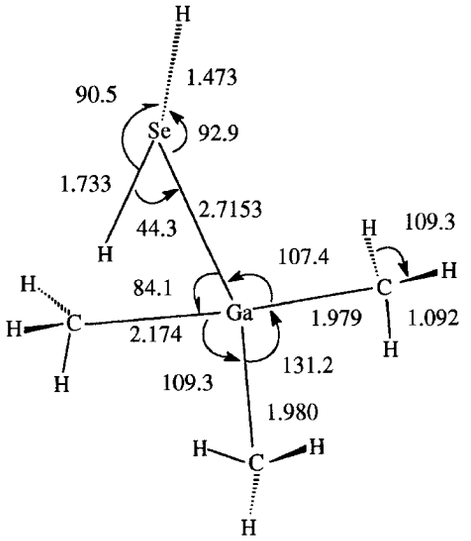


**Fig. 4** Density functional theory (DFT) structure for the $Me_3Ga$–$H_2Se$ transition state calculated at the B3LYP/6-311G(d,p)//B3LYP/6-311G(d,p) level of theory. The bond lengths are in Å and the bond angles in degrees. Energies are given in Table 1.

an order of magnitude increase in the value of the rate constant for reaction (R2c), [$k_{298}$(R2c)].

We therefore propose that the reaction mechanism consists of (R2c) followed by (R3) and (R6) since transient formation of an $Me_2Ga$–SeH intermediate followed by rapid polymerisation to involatile polymer species as postulated in reaction (R6) will lead to rapid depletion of $GaMe_3$ from the gas phase.

Using a thermodynamic analysis, developed previously for the reaction of $GaMe_3$ with $H_2Se$ as a function of growth temperature,[3] we have also modelled the extent of reaction as a function of VI/III ratio at room temperature assuming the MOCVD reactor to be a closed isothermal system at equilibrium. Although included in the calculation the hydrogen mol fraction is excluded from the plot since it is always close to unity. The results for a constant $GaMe_3$ mol fraction and varying $H_2Se$ mol fraction are shown in Fig. 5. The extent of reaction at VI/III > 1 is significant consuming virtually all the input $GaMe_3$ at VI/III ≥ 2. The dominant solid phase is $Ga_2Se_3$ for VI/III ratios in excess of 1.1. At VI/III *ca.* 1 GaSe is the dominant solid phase. The simulated extent of reaction with VI/III < 1 is as expected, showing less variation than for VI/III > 1 since the large excess of $GaMe_3$ reduces the importance of the depletion reaction on the total $GaMe_3$ concentration.

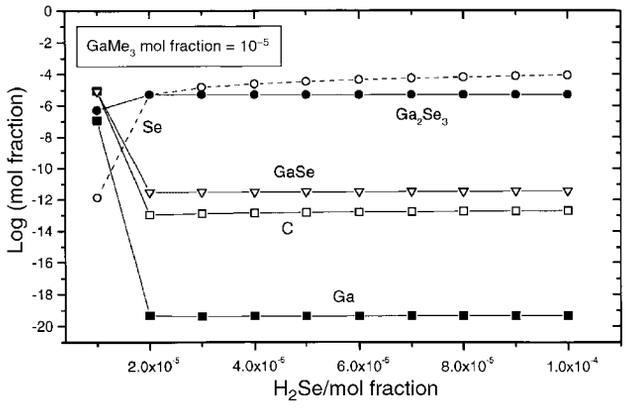


**Fig. 5** Dependence of the equilibrium mol fractions in the gas phase for the $GaMe_3$–$H_2Se$–$H_2$ system. Results are calculated for a pressure of 1.0 atm at 298 K. (The hydrogen mol fraction is excluded since it is always close to unity.) Thermodynamic simulation of growth at a fixed $GaMe_3$ mol fraction ($1.0 \times 10^{-5}$) but with varying $H_2Se$ mol fraction.

GaSe is the dominant solid phase for all VI/III < 1 with $Ga_2Se_3$ a minor product.

Kinetic simulations[31] of the growth mechanism using the computed thermochemical kinetic data allowed the extent of the reaction occurring under typical growth conditions to be investigated as a function of reactor residence time (∝ 1/reactor pressure). As Fig. 6 shows, it is predicted that the pre-deposition reaction will not be significant for reaction times as small as $10^{-3}$ s corresponding to reactor pressures ≤ 1 Torr. Clearly, very low pressure operation would be of benefit in improving the quality of the growth of gallium selenides using this particular precursor combination.

The simulation also predicts that the intermediate species $Me_2Ga$–SeH is produced very rapidly on mixing $GaMe_3$ and $H_2Se$; the maximum in the concentration of $Me_2Ga$–SeH is achieved after only 0.1 s, and thereafter decays assymptotically to zero (effectively the reaction is complete after 18 s). Concomitant with the drop in the $GaMe_3$ and $H_2Se$ concentrations and the rise and fall in the $Me_2Ga$–SeH concentration the transformation of the precursor to the final polymer product, *i.e.* MeGa=Se, reaches a maximum after 0.3 s and thereafter decays assymptotically to zero. Since, the enthalpy change for the formation of the dimer $(MeGa–Se)_2$ from MeGa=Se is exothermic, it is assumed that the activation barrier to the formation of the polymer species $(MeGa–Se)_n$, is small and since the rate of MeGa=Se production is not rate determining, polymerisation is facile. Although the participation of the intermediate species, $Me_2Ga$–SeH and MeGa=Se, is at present inferred from theoretical calculations and not yet experimentally confirmed, we believe that both the experimental[10] and theoretical[14] evidence against the involvement of any stable adduct species in the growth process is convincing, while the growth of an amorphous layer containing Ga and Se at room temperature clearly argues against independent thermal decomposition of the $GaMe_3$ and $H_2Se$ precursors as a route to film deposition. Experimental confirmation of proposed reaction intermediates will have to await further investigation using non-invasive FTIR absorption spectroscopy.[32] Examination of $Ga_2Se_3$ layers grown on both (001) GaAs and (001) GaP substrates at $T_g > 450$ °C using transmission electron microscopy has indicated that film morphology and structure[6] is compromised by this low temperature reaction which still occurs at these elevated temperatures in the presence of the desired epitaxial growth processes. In contrast, the structural properties obtained using the dialkylselenium source di-*tert*-butylselenide, where the pre-deposition reaction is absent, are significantly improved.

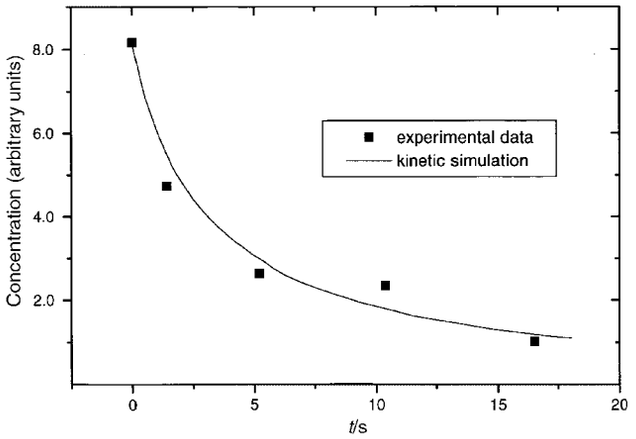


**Fig. 6** Kinetic simulation of the pre-deposition reaction between $GaMe_3$ and $H_2Se$ at atmospheric pressure and 298 K. The calculation assumes an input molar ratio of $GaMe_3$ : $H_2Se$ of 1 : 1 with rate parameters computed from DFT and canonical transition state theory (CTST).[31]

## Conclusions

We have used a simple mass spectrometer sampling system, in conjunction with a conventional atmospheric pressure MOCVD reactor to study, for the first time, the kinetics of the room temperature reaction between $GaMe_3$ and $H_2Se$. The reaction appears to go to completion within 18 s of mixing in the inlet region of the reactor; a white/buff coloured deposit of possibly polymeric material containing Ga and Se in the ratio 1 : 1 along with a measurable but unknown amount of carbon was deposited and methane was the only volatile reaction product detected. We have shown by a combination of experimental results and theoretical calculations that the spontaneous reaction between $GaMe_3$ and $H_2Se$ is consistent with a homogeneous mechanism which proceeds through a $Me_2Ga$–SeH intermediate. Clearly, a Se precursor which does not contain abstractable H atoms (Se–H bonds) is needed if deposition of gallium selenides at atmospheric pressure without parasitic reactions is desired.

## Acknowledgements

We would like to thank the Engineering and Physical Sciences Research Council (EPSRC) for supporting aspects of this work and the Higher Education Funding Council for Wales (HEFCW) for provision of a Silicon Graphics R10000 workstation.

## References

1 N. Teraguchi, F. Kato, M. Konagai and K. Takahashi, *Jpn. J. Appl. Phys.*, 1989, **28**, L2134.
2 J. O. Williams, N. Maung, A. C. Wright, *Metal–Organic Chemical Vapour Deposition (MOCVD) for the Preparation of New Materials and Devices*, in *IUPAC Monographs on Chemistry for the 21st Century: Interfacial Science*, Blackwell Science Ltd., Oxford, 1997.
3 N. Maung, G. H. Fan, T. L. Ng, J. O. Williams and A. C. Wright, *J. Cryst. Growth*, 1996, **158**, 68.
4 D. Morley, M. von der Emde, D. R. T. Zahn, V. Offerman, T. L. Ng, N. Maung, A. C. Wright, G. H. Fan, I. B. Poole and J. O. Williams, *J. Appl. Phys.*, 1996, **79**, 3196.
5 M. von der Emde, D. R. T. Zahn, T. L. Ng, N. Maung, G. H. Fan, I. B. Poole, J. O. Williams and A. C. Wright, *Appl. Surf. Sci.*, 1996, **104**, 575.
6 T. L. Ng, N. Maung, G. H. Fan, I. B. Poole, J. O. Williams and A. C. Wright, *Adv. Mater.*, 1996, **2**, 185.
7 G. H. Fan, N. Maung, T. L. Ng, P. F. Heelis, J. O. Williams, A. C. Wright, D. F. Foster and D. J. Cole-Hamilton, *J. Cryst. Growth*, 1997, **170**, 485.
8 A. C. Jones and P. O'Brien, *The Chemistry of Compound Semiconductor CVD—Preparation and Uses*, VCH, Weinheim, 1997.
9 G. E. Coates, M. L. H. Green and K. Wade, *Organometallic Compounds*, Methuen, London, 3rd edn., 1967, vol. 1.
10 E. A. Piocos and B. S. Ault, *J. Am. Chem. Soc.*, 1989, **111**, 8978.
11 E. A. Piocos and B. S. Ault, *J. Phys. Chem.*, 1991, **95**, 6827.
12 E. A. Piocos and B. S. Ault, *J. Phys. Chem.*, 1992, **96**, 7589.
13 H. Bai and B. S. Ault, *J. Phys. Chem.*, 1994, **98**, 6082.
14 N. Maung, *J. Mol. Struct. (THEOCHEM)*, 1998, **432**, 129.
15 M. R. Czerniak and B. C. Easton, *J. Cryst. Growth*, 1984, **68**, 128.
16 J. S. Whiteley and S. K. Ghandhi, *J. Electrochem. Soc.*, 1983, **130**, 1191.
17 P. D. Agnello and S. K. Gandhi, *J. Electrochem. Soc.*, 1988, **135**, 1530.
18 G. P. Smith and R. Patrick, *Int. J. Chem. Kinet.*, 1983, **15**, 167.
19 W. J. Hehre, L. Radom, P. R. v. Schleyer and J. A. Pople, *Ab Initio Molecular Orbital Theory*, John Wiley & Sons, New York, 1986.
20 R. G. Parr and Y. Weitao, *Density-Functional Theory of Atoms and Molecules*, Oxford University Press, Oxford, 1995.
21 J. M. Seminario and P. Politzer, *Modern Density Functional Theory: A Tool for Chemistry*, Elsevier, Amsterdam, 1995.
22 GAUSSIAN 94 (Revision E.1), M. J. Frisch, G. W. Trucks, H. B. Schlegel, P. M. W. Gill, B. C. Johnson, M. A. Robb, J. R. Cheeseman, T. A. Keith, G. A. Petersson, J. A. Montgomery, K. Raghavachari, M. A. Al-Laham, V. G. Zakrzewski, J. V. Ortiz, J. B. Foresman, J. Cioslowski, B. B. Strefanov, A. Nanayakkara, M. Challacombe, C. Y. Peng, P. Y. Ayala, W. Chen, M. W. Wong, J. L. Andres, E. S. Replogle, R. Gomperts, R. L. Martin, D. J. Fox, J. S. Binkley, D. J. Defrees, J. Baker, J. P. Stewart, M. Head-Gordon, C. Gonzalez and J. A. Pople, Gaussian Inc., Pittsburgh, PA, 1995.
23 SPARTAN version 4.1.2, Wavefunction Inc., 18401 Von Karman Ave., #370, Irvine, CA 92715, U.S.A., ©1995 Wavefunction, Inc.
24 W. J. Hehre, L. D. Burke, A. J. Shusterman and W. J. Pietro, *Experiments in Computational Organic Chemistry*, Wavefunction, Inc. Irvine, 1993.
25 W. J. Hehre, *Practical Strategies for Electronic Structure Calculations*, Wavefunction, Inc., Irvine, 1995.
26 W. J. Hehre, A. J. Shusterman and W. W. Huang, *A Laboratory Book of Computational Organic Chemistry*, Wavefunction, Inc., Irvine, 1996.
27 *The Molecular Modeling Workbook for Organic Chemistry*, ed. W. J. Hehre, A. J. Shusterman and J. E. Nelson, Wavefunction, Inc., Irvine, 1998.
28 GAUSSIAN 94 (Revision D.1 and higher) User's Reference, Gaussian Inc., Pittsburgh, PA, 1994–1996.
29 J. B. Foresman and A. E. Frisch, *Exploring Chemistry with Electronic Structure Methods*, Gaussian Inc., Pittsburgh, PA, 2nd edn., 1995–1996.
30 E. Wigner, *Z. Phys. Chem.*, 1932, **19**, 203.
31 J. I. Steinfeld, J. S. Francisco and W. L. Hase, *Chemical Kinetics and Dynamics*, Prentice-Hall, Englewood Cliffs, NJ, 1989.
32 S. Salim, C. A. Wang, R. D. Driver and K. F. Jensen, *J. Cryst. Growth*, 1996, **169**, 443.

*Paper 9/02688F*